# Origins of extreme broadening mechanisms in near-edge x-ray spectra of nitrogen compounds

John Vinson, Terrence Jach, W. T. Elam, and J. D. Denlinger

Phys. Rev. B **90**, 205207 — Published 10 November 2014

DOI: 10.1103/PhysRevB.90.205207

# Origins of Extreme Broadening Mechanisms in Near-edge X-ray Spectra

John Vinson and Terrence Jach
*Material Measurement Laboratory, National Institute of Standards and Technology, Gaithersburg, MD 20899*

W. T. Elam
*Applied Physics Laboratory, University of Washington, Seattle, WA 98195*

J. D. Denlinger
*Advanced Light Source, Lawrence Berkeley National Laboratory, Berkeley, CA 94720*

(Dated: October 3, 2014)

We demonstrate the observation of many-body lifetime effects in valence-band x-ray emission. A comparison of the N K$\alpha$ emission of crystalline ammonium nitrate to molecular orbital calculations revealed an unexpected, extreme broadening of the NO $\sigma$ recombination – so extensively as to virtually disappear. $GW$ calculations establish that this disappearance is due to a large imaginary component of the self-energy associated with the NO $\sigma$ orbitals. Building upon DFT, we have calculated radiative transitions from the nitrogen 1$s$ level of ammonium nitrate and ammonium chloride using a Bethe-Salpeter method to include electron-hole interactions. The absorption and emission spectra of both crystals evince large, orbital-dependent sensitivity to molecular dynamics. We demonstrate that many-body effects as well as thermal and zero-point motion are vital for understanding observed spectra. A computational approach using average atomic positions and uniform broadening to account for lifetime and phonon effects is unsatisfactory.

PACS numbers: 78.70.Dm, 78.70.En, 71.15.Qe

## I. INTRODUCTION

Fundamental to our understanding of electronic excitations is the notion of the quasiparticle. As per Landau, under certain conditions many-body excitations can be treated as single-particle excitations of quasiparticles, retaining fundamental properties like quantum numbers, but with shifted energies or effective masses due to many-body interactions. Crucially, quasiparticles are excitations with a finite lifetime which spectroscopically is manifest as an energy broadening. Variations in lifetime broadening of deeply-bound core levels are well known,[1] but heretofore the conduction and valence band lifetimes have been either found or assumed to be uniform and long. For the first time we definitively show evidence of many-body lifetime broadening in valence x-ray emission, uniquely contributing to the observed "disappearance" of the NO $\sigma$ peak in $NH_4NO_3$. The anomalously short lifetime of these orbitals pushes against the underlying assumption of a long-lived quasiparticle.

Recently we identified the features of N 1$s$ emission spectra from several crystalline, insulating compounds using molecular orbital (StoBe) and real-space Green's function theories (FEFF).[2] While these calculations showed sufficient similarity to observed spectra that bond assignments could be made, quantitative agreement was poor; the fluorescence from NO $\sigma$ bonds in $NH_4NO_3$ was greatly broadened in the experimental spectrum, an effect not captured by the theoretical calculations. The N K-edge spectra of other nitrate salts have been previously investigated, and, while some evidence of NO $\sigma$ broadening is present, only rough interpretations were made via the structure of the nitrate ion.[3–5] Calculations of x-ray spectra of molecules and molecular solids have also demonstrated the importance of considering initial-state thermal atomic disorder on local valence states using molecular dynamics with classical nuclei,[6–9] and zero-point disorder in liquids.[10,11]

Here we present x-ray absorption (XAS) and emission spectra (XES) for $NH_4NO_3$ ammonium nitrate (AN) and $NH_4Cl$ ammonium chloride (AC), reexamining previous AN measurements.[2] AN provides a useful test bed for crystalline molecular solids, containing both a strongly reduced and strongly oxidized nitrogen, in different geometries, in a relatively small unit cell. This diversity leads to different phonon coupling and electronic structure, the effects of which are interleaved in the observed spectra. AC allows for the isolation of the ammonium ion and the separation of those effects which originate from molecular dynamics versus those which originate from electronic correlations. We calculated near-edge x-ray spectra using a $GW$/Bethe-Salpeter equation (BSE) formalism developed within the OCEAN code.[12] Standard calculation methods utilize a frozen atomic configuration and parameterize phonon and lifetime broadening as *ad hoc* terms adjusted to best match experiment. Here we eschew system-dependent fitting and incorporate a $GW$-based, complex-valued self-energy and quantum nuclear disorder. Both of these effects are required to bring about agreement between calculations and observed data.

## II. EXPERIMENT

We obtained x-ray absorption and x-ray emission spectra on the spectroscopy undulator beamline 8.0.1 at the

Advanced Light Source. The beamline is comprised of a focusing spherical grating monochromator and a spherical grating spectrometer on a Rowland circle with a microchannel plate detector.[13] The samples are measured in ultra-high vacuum. We calibrated the monochromator using the N K-absorption spectrum of $N_2$ gas embedded in ZnO by ion implantation. Multiple vibrational bands were fitted assuming the value for the first vibrational peak corresponding to the initial $1s$–$1\pi_g^*$ band transition of 400.70 eV.[14] The standard uncertainty of monochromator energy from the fit to the bands was 0.08 eV. XES and elastic scattering from $N_2$ were used to calibrate the emission spectrometer with an uncertainty of $\pm 0.2$ eV. Samples of AC and AN were prepared by pressing the microcrystalline powder (99.89% purity) into indium foil. The absorption spectra were obtained by two methods: measuring the total sample current and integrating the total spectrometer yield. The results were essentially identical. The absorption spectra were obtained in steps of 0.1 eV with 0.5 s intervals.

A small sharp feature observed around 401 eV in the absorption spectrum of AC and AN was due to $N_2$ present in the powder.[15] We were conscious that the x-ray beam could induce a change in oxidation state that we have observed between $NaNO_2$ and $NaNO_3$,[5] an effect that grows with exposure time. The spectra here did not reveal any such changes, and the reduction products in this case are generally volatile. We are confident that the emission spectra reflect only the presence of the original compounds.

The emission spectra were obtained by excitation with the incident beam tuned near 417 eV for AC and 422 eV for AN. These energies were sufficiently high that correlation effects between absorption and emission were minimized, and the oscillator strength of emission was not a sensitive function of the excitation energy. The samples were located on a Rowland circle that included a spherical grating with a pitch of 1500 lines/mm and a position-sensitive microchannel plate to collect the photons.[13] The acceptance of the microchannel plate covered an energy range of 40 eV over 512 channels. The entire emission spectrum from the valence band was thus recorded all at once. The total recording times for the AC and AN were 300 s and 1800 s, respectively. All measurements were made at room temperature.

## III. THEORY

The OCEAN package provides accurate descriptions of many systems including liquid and solid $H_2O$[16] as well as $L_{2,3}$ edges of early transition metals.[17] Details can be found in Ref. 12. In low-Z nuclei, Auger decay is the primary decay channel for $1s$ holes. We neglect excitation energy and material dependence of the Auger decay rate and take the core-hole lifetime to be 0.1 eV.[18] Because of the fast Auger decay rate, OCEAN treats the ions as frozen during both absorption and emission processes, and the resulting spectrum is a function of the initial atomic configuration only. Furthermore, the XES is taken to be decoupled from the initial excitation.

The ground-state electronic structures were computed using the local-density approximation (LDA) to density-functional theory (DFT) using QUANTUMESPRESSO.[19] Sampling of the Brillouin zone used an interpolation scheme.[20,21] For both absorption and emission we average over orthogonal polarizations as well as each nitrogen site $i$ in the cell, accounting for chemical shifts according to $\Delta E_i = \epsilon_{1s} + V_{KS}(\tau_i) - 1/2W(\tau_i)$, where $V_{KS}$ is the total Kohn-Sham potential and $W$ is the screened core-hole potential, both evaluated at core-hole site $\tau_i$. The parameter $\epsilon_{1s}$ is a constant for different ionic distributions within the same cell and is chosen to align the calculated XAS with experiment. While this does not give absolute alignment, it correctly accounts for relative chemical shifts across different configurations of a disordered system.[16,22] XAS and XES use the same $\epsilon_{1s}$, and so their spacing is not a free parameter.

While calculations often use average or "frozen" atomic coordinates, the physical sample is always in a semi-disordered state due to vibrations from both thermal and zero-point motion. To model this we constructed configurations by populating the phonon modes of the crystal at 295 K. Two classes of structures were created; for the first we used thermal occupancies ("Semi-classical"), while for the second we included the additional 1/2 quantum per mode of zero-point energy ("Quantum"). The displacement of each atom $\Delta\tau_\alpha$ is determined as follows. 1) We calculated the phonon modes $\{\xi_\lambda\}$ and energies $\{\omega_\lambda\}$ by diagonalizing the dynamical matrix $D$ on a $4\times4\times4$ $k$-point grid using density-functional perturbation theory as implemented in QUANTUMESPRESSO[23] and projecting it onto a $2\times2\times2$ supercell. The dynamical matrix is the partial derivative of the force on atom $\alpha$ with respect to the displacement of atom $\beta$ evaluated at their equilibrium positions. 2) Treating each phonon mode as a quantum harmonic oscillator, the mode-dependent displacement variances $\langle u^2\rangle_{\alpha,\lambda}$ for each ion were calculated. 3) Every mode was assigned a normally-distributed random value $g_\lambda$, and ionic displacements were determined by summing over modes.

$$\begin{aligned} &D\,\xi_\lambda = \xi_\lambda\,\omega_\lambda^2 \\ &D_{\alpha\beta} \equiv (m_\alpha m_\beta)^{-1/2}(-\partial F_\alpha/\partial R_\beta)_{R_0} \end{aligned} \tag{1}$$

$$\langle u^2\rangle_{\alpha,\lambda} = \frac{\vec{\xi}_{\alpha,\lambda}\cdot\vec{\xi}_{\alpha,\lambda}}{\omega_\lambda\, m_\alpha} \begin{cases} n(\omega_\lambda;T) & \text{Semi-classical} \\ 1/2 + n(\omega_\lambda;T) & \text{Quantum} \end{cases} \tag{2}$$

$$\Delta\tau_\alpha = \sum_\lambda g_\lambda\,\hat{\xi}_{\alpha,\lambda}\sqrt{\langle u^2\rangle_{\alpha,\lambda}} \tag{3}$$

where $n(\omega;T)$ is the Bose occupation for phonons of energy $\omega$ at temperature $T$. This was repeated with new sets $\{g_\lambda\}$ to construct each structure, and the theoretical spectra are the result of averaging over several configurations.

The use of DFT orbitals for excited-state calculations

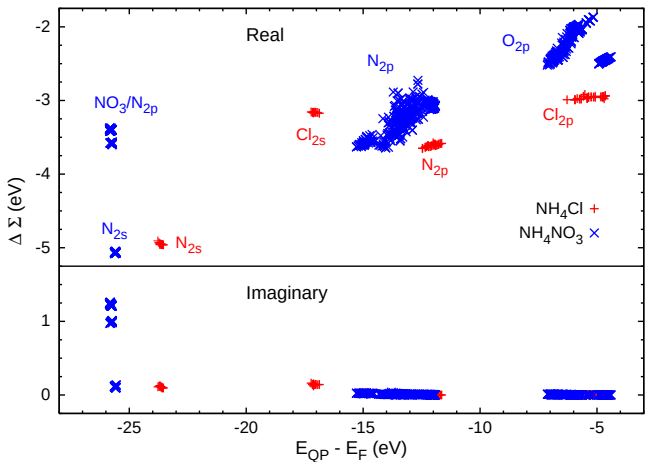


FIG. 1. (color online) The real (top) and imaginary (bottom) components of the self-energy corrections for the occupied states of $NH_4Cl$ and $NH_4NO_3$. Labels denote the majority character of the states. The states with large broadening near -26 eV are NO $\sigma$ orbitals. This anomalously large imaginary self-energy has a profound effect on the XES (Fig. 3a).

is made rigorous by way of self-energy corrections,[24] which we have carried out within the $GW$ approximation using ABINIT.[25,26] In a condensed system, electron or hole excitations are screened, creating a quasiparticle with both a shift in energy and a finite broadening when many-body interactions are considered. This is referred to as the self-energy $\Sigma$, and the imaginary component is related to the quasiparticle's linewidth or lifetime: $1/2\tau^{-1} = \Gamma \approx \mathrm{Im}[\Sigma]$. This lifetime can be seen experimentally, *e.g.,* band broadening in photo-emission. For the systems we are investigating here the DFT orbitals serve as good surrogates, and we therefore updated the energies only. The self-energy calculations were carried out for the frozen unit cell, and $k$-point averaged corrections were applied to the energies band-by-band:

$$E_{nk} = E^{\mathrm{LDA}}_{nk} + \Re e[\Delta\Sigma_n] + i\Im m[\Delta\Sigma_n].$$

This form however assumes that the broadening is small, and we underestimate the smearing of states whose spectral function does not match a Lorentzian lineshape. Our $GW$ calculations overestimate the band gap of both materials, which we attribute to a neglect of wavefunction relaxation. Numerical details are given in the appendix.

## IV. RESULTS

### A. Ammonium Chloride

AC allows us to isolate the behavior of the ammonium cation. It crystallizes in a cubic CsCl lattice. At room temperature the alignment of the hydrogen atoms is fully disordered, giving a P$m3m$ structure, but below -30 C there is a phase transition to the hydrogen-ordered P$\bar{4}3m$ phase.[27,28] We expect little effect on the x-ray spectra from this phase transition, *cf.*, high-density ice,[29] and therefore we based our calculations on the ordered phase. We used the room-temperature, experimentally determined lattice parameter of 3.866 Å and set the hydrogen positions by minimizing the forces calculated within DFT.[27] The average mean displacements were found to be in good agreement with experiment.[30] All calculated spectra for AC and AN include an approximate core-hole lifetime broadening of 0.1 eV that accounts for both radiative and Auger decay, and an experimental broadening of 0.2 eV and 0.5 eV for the absorption and emission, respectively.

The calculated self-energy corrections gave a direct band gap of 9.30 eV compared to the LDA value of 4.60 eV and experimental value of approximately 7.8 eV at 77 K.[31] Nuclear disorder reduces the gap, and our configurations had $GW$-corrected gaps around 7.8-8.3 eV. The self-energy corrections are shown in figure 1, and the occupied states form distinct groups. The corrections change the spacing of these groups but are not a significant source of broadening for either absorption or emission. The XAS is minimally affected by the $GW$ corrections so we apply them only to the emission.

The gross features of the AC nitrogen K$\alpha$ emission and K-edge absorption are captured by the OCEAN code using the frozen structure (Fig. 2), but there are notable discrepancies. The absorption spectrum shows a general broadening with disorder, but the excitonic feature at 406 eV is overly broadened in our calculation. Compared to the observed spectra, the calculated emission gives incorrect relative weights and spacing between the two features, and the dominant peak near 390 eV is too narrow. The introduction of disorder using either semi-

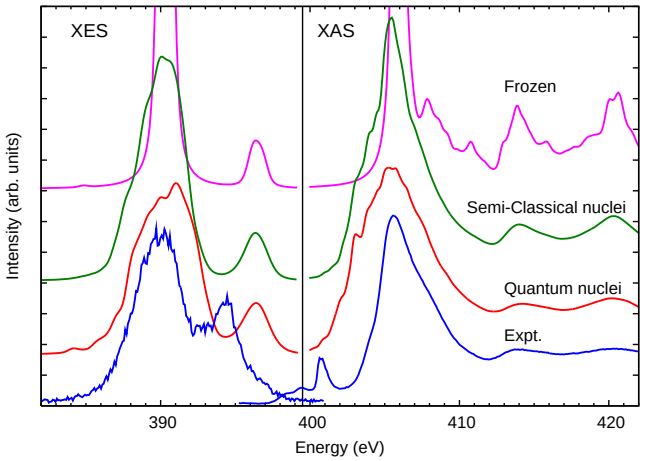


FIG. 2. (color online) The nitrogen K-edge emission (left) and absorption spectra (right) of $NH_4Cl$ calculated using various approximations (see text) and compared to experiment. All three calculated XES use $GW$-corrected energies. Spectra are offset vertically for clarity.

classical or quantum nuclei has a dramatic effect on the resulting emission spectra. The main feature consists of $sp^3$ states centered on the nitrogen, and with disorder we capture its strong, asymmetric broadening. The secondary peak shows little broadening with disorder, but we note an increase in its relative strength with zero-point motion.

Our method over-broadens the main emission peak and fails to correct the position of the secondary which we suggest is a limitation of using initial-state vibrational disorder. Despite the short core-hole lifetime, some atomic relaxation will occur, especially for hydrogen atoms.[32] The position of the secondary peak is sensitive to the NH bond length, moving significantly lower in energy as the bond lengthens – the expected movement of the hydrogen atoms in response to the positive core hole.

### B. Ammonium Nitrate

AN forms a P$mmn$ structure at room temperature.[33] Using the experimentally determined structure we calculated a $GW$ gap of 8.80 eV compared to the LDA value of 3.24 eV, but nuclear disorder reduced this by ∼1 eV. We estimate an optical gap of 5.9 eV based on comparison with other nitrate salts.[34] Recent DFT calculations hypothesized a slight deformation giving a P$mn2_1$ structure.[35] We suggest this corresponds to extreme mode softening in the $NO_3$, but to avoid instabilities in the phonon calculation we have used this distorted structure optimized within DFT. After accounting for the two-fold degeneracy in the structural deformation of the nitrate groups, the thermal parameters were found to be in decent agreement with experiment.[36]

We show the XES of AN in figure 3a, and, using the frozen nuclear coordinates, we confirm earlier calculations.[2] With thermal and then also zero-point disorder we see additional broadening in both the $NH_4$ peak at 390 eV and the $NO_3$ $\sigma$ peak at 382 eV. $GW$ corrections further broaden the $NO_3$ $\sigma$ peak, which appears broadened even more in the experiment (see appendix A). The higher-energy $NO_3$ $\pi$ bonds at 394 eV are largely unaffected by vibrations. The experimental data however show a much broader structure for this peak or a doublet separated by 1 eV. It is possible that the additional smearing of both $NO_3$ peaks has the same cause, possibly from some mixture of structures present in the sample or excited-state phonon effects causing additional distortions in the $NO_3$. A weak peak near 400 eV is well reproduced by our calculation after being broadened by the disorder and shifted by the self-energy.

The self-energy unexpectedly shows a large correction associated with N $p$ levels of the nitrate ion (Fig. 1) in stark contrast to AC which shows a more generic smooth, slow growth in the imaginary part of the self-energy with binding energy. The lifetime of a quasiparticle excitation is inversely related to its probability of scattering into

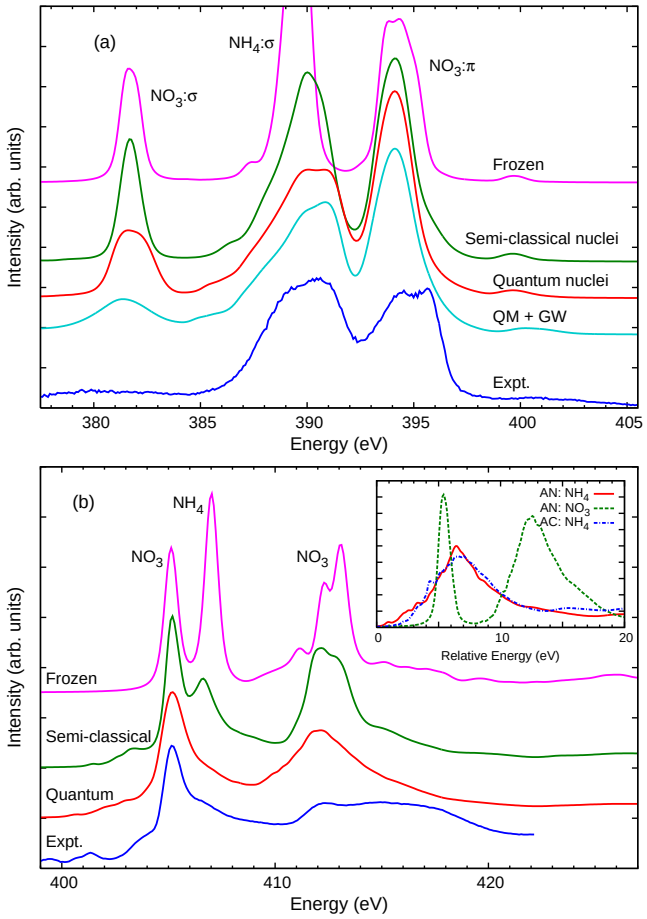


FIG. 3. (color online) The nitrogen K-edge emission (top) and absorption (bottom) spectra of $NH_4NO_3$ calculated using various configurations (see text) and compared to experiment. The inset shows the separate contributions of $NH_4$ and $NO_3$ for AN and AC with quantum disorder. *N.B.* The XES experimental data was previously published in Ref. 2.

other states. A quasihole $i$ can deexcite into state $f$ by promoting a valence electron $v$ into a conduction-band state $c$ via the screened Coulomb interaction $W$. The lifetime $\tau_i$ is approximately

$$\tau_i^{-1} \propto \sum_{c,v,f} |\langle i,v|W|f,c\rangle|^2 \delta\left((\epsilon_c - \epsilon_v) - (\epsilon_f - \epsilon_i)\right),$$

neglecting exchange and self-consistency. We see imediately that the energy difference $\epsilon_f - \epsilon_i$ must be greater than the band gap, and that the colocation of states $i$ and $f$ will enhance the strength of the matrix element. The planar structure of $NO_3$ splits the occupied $p$ orbitals into $\pi$ and more-bound $\sigma$ states. Their ∼13 eV splitting is well above AN's band gap, leading to a reduced lifetime and the orbital-specific broadening responsible for the unique "disappearance" of the $\sigma$ NO peak in the x-ray emission of AN.[2]

In the calculated absorption (Fig. 3b) the features at 405 eV and 412 eV arise from the nitrate and are anal-

ogous to the structures seen in $LiNO_3$ and $NaNO_3$,[3,4] whereas the sharp peak at 407 eV arises from the ammonium, similar to AC (see inset). The addition of zero-point motion results in substantial broadening of this feature and moves it lower in energy, becoming both the shoulder of the nitrate exciton and the pre-edge feature, whereas the semi-classical structures give a clearly-separated $NH_4$ peak contrary to experimental observation. In contrast, the nitrate exciton at 405 eV is positioned in the empty spaces above and below the planar $NO_3$, isolated from the effects of atomic disorder. The residual shoulder in the measured spectrum between 415 eV and 420 eV is likely due to incomplete control of background or secondary excitations. In this energy range a photon can excite the $NO_3$ exciton plus an additional valence electron-hole pair, and such effects are not present in our calculation.

## V. CONCLUDING REMARKS

In summary, we have considered the nitrogen K$\alpha$ emission and K-edge absorption of two large-gap, ionic insulators: ammonium chloride and ammonium nitrate. We found that an accurate description of these materials requires accounting for self-energy effects and large atomic motion (including zero-point vibrations). Many-body effects lead to unique broadening of a portion of the emission spectra of AN. This broadening of the NO $\sigma$ bonds should be generic to $NO_3^-$, e.g., $LiNO_3$.[3] We suggest that the requirements for observing this anomalous broadening in other materials are two-fold: 1) a splitting in the occupied states by way of lone-pairs or highly asymmetric bonds, and 2) the splitting is large enough that a decay from lower to upper can promote excitons across the gap. With small core-hole and experimental broadenings XES of light elements can allow for the precise determination of valence-band quasiparticle lifetimes of bulk materials, serving as a check on calculations.

Our method over-broadens the ammonium-derived peaks, and at present there has been no accounting for excited-state phonon effects; specifically during the x-ray excitation there will be some amount of ionic relaxation due to the core hole.[22,37–39] Coupling of x-ray excitations to vibrational modes is well-studied in molecules, *e.g.*, Ref. 40, where the paucity of modes and large distortions from dissociation leave clear markers of vibrational excitations. Future work should include vibrational dynamics during the core-excited state in crystalline and extended systems.

## ACKNOWLEDGMENTS

This work was supported in part by the Office of Naval Research under grant N00014-05-1-0843 (WTE). The Advanced Light Source is supported by the Director, Office of Science, Office of Basic Energy Sciences, of the U.S. Department of Energy under Contract No. DE-AC02-05CH11231. The authors wish to thank Dr. Eric Shirley for helpful discussions. Certain software packages are identified in this paper to foster understanding. Such identification does not imply recommendation or endorsement by the National Institute of Standards and Technology, nor does it imply that these are necessarily the best available for the purpose.

### Appendix A: Ammonium Nitrate Emission

In the nitrogen K$\alpha$ emission from ammonium nitrate the two main peaks, $NH_4$ $\sigma$ and $NO_3$ $\pi$, dwarf contributions from the NO $\sigma$ and valence states. In figure 4 below we include a cropped version of the experimental spectrum shown in figure 3a. While the NO $\sigma$ contribution is quite broad, it is clearly distinct from the background.

### Appendix B: GW calculations

The *GW* calculations were carried out using the ABINIT code.[25,26] We used the Fritz-Haber (.fhi)[41] pseudopotentials available from the ABINIT website (www.abinit.org). These are norm-conserving Troiller-Martins,[42] using the Perdew-Wang style of LDA.[43] For both AN and AC we used a $4^3$ $\Gamma$-centered $k$-point grid to calculate the screening and self-energy giving 27 and 10 points in the irreducible Brillouin zone respectively. For both we iterated 4 times, updating the energies, but not the wavefunctions. Several of the settings used are in excess of what is necessary for accurate calculations.

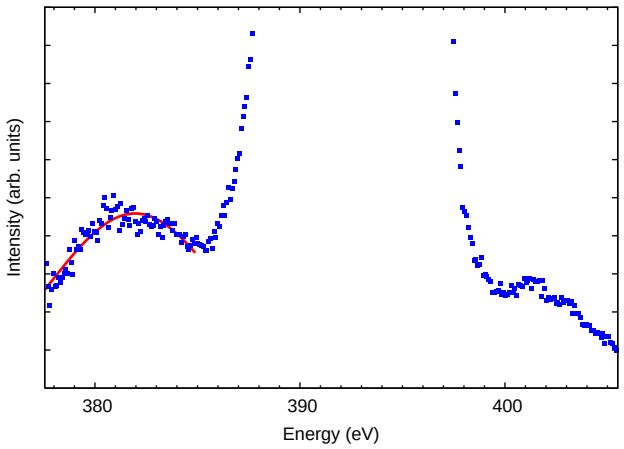


FIG. 4. The experimental emission of $NH_4NO_3$ (fig. 3a) cropped to better show the NO $\sigma$ peak at 382 eV and valence peak at 400 eV. The central region contains both the $NH_4$ $\sigma$ and $NO_3$ $\pi$ peaks. The red line is a best-fit Gaussian with a FWHM of 10 eV to aid the eye.

### 1. $NH_4Cl$

We included 400 unoccupied bands for the screening and used a 12 Ha. cutoff for the dielectric matrix. We caculated 80 real and 10 imaginary frequencies using ABINIT's tangential grid function with a halfway mark of 25 eV and the default maximum. The wavefunctions were sampled down to 16 Ha. We calculated corrections for the first 32 bands, and used a 20 Ha. cutoff for the exchange part of the self-energy operator.

### 2. $NH_4NO_3$

We included 480 unoccupied bands for the screening and used an 8 Ha. cutoff for the dielectric matrix. We caculated 30 real and 10 imaginary frequencies using ABINIT's tangential grid function with a halfway mark of 10 eV and a maximum of 30 eV. The wavefunctions were sampled down to 15 Ha. We calculated corrections for the first 64 bands, and used a 40 Ha. cutoff for the exchange part of the self-energy operator.

[1] P. H. Citrin, Phys. Rev. Lett. **31**, 1164 (1973).
[2] F. D. Vila, T. Jach, W. T. Elam, J. J. Rehr, and J. D. Denlinger, J. Phys. Chem. A **115**, 3243 (2011).
[3] A. B. Preobrajenski, A. S. Vinogradov, S. A. Krasnikov, R. Szargan, and N. Mårtensson, Phys. Rev. B **69**, 115116 (2004).
[4] A. B. Preobrajenski, A. S. Vinogradov, S. L. Molodtsov, S. K. Krasnikov, T. Chassé, R. Szargan, and C. Laubschat, Phys. Rev. B **65**, 205116 (2002).
[5] A. S. Vinogradov, A. B. Preobrajenski, S. L. Molodtsov, S. A. Krasnikov, R. Szargan, A. Knop-Gericke, and M. Hävecker, Chem. Phys. **249**, 249 (1999).
[6] J. S. Uejio, C. P. Schwartz, R. J. Saykally, and D. Prendergast, Chem. Phys. Lett. **467**, 195 (2008).
[7] C. P. Schwartz, R. J. Saykally, and D. Prendergast, J. Chem. Phys. **133**, 044507 (2010).
[8] F. D. Vila, J. J. Rehr, S. D. Kelly, and S. R. Bare, J. Phys. Chem. C **117**, 12446 (2013).
[9] F. Vila, J. J. Rehr, J. Kas, R. G. Nuzzo, and A. I. Frenkel, Phys. Rev. B **78**, 121404 (2008).
[10] L. Kong, X. Wu, and R. Car, Phys. Rev. B **86**, 134203 (2012).
[11] M. P. Ljungberg, J. J. Mortensen, and L. G. M. Pettersson, J. Electron Spectrosc. Relat. Phenom. **184**, 427 (2011).
[12] J. Vinson, J. J. Rehr, J. J. Kas, and E. L. Shirley, Phys. Rev. B **83**, 115106 (2011).
[13] J. J. Jia, T. A. Callcott, J. Yurkas, A. W. Ellis, F. J. Himpsel, M. G. Samant, J. Stöhr, D. L. Ederer, J. A. Carlisle, E. A. Hudson, et al., Rev. Sci. Instrum. **66**, 1394 (1995).
[14] A. P. Hitchcock and C. E. Brion, J. Electron Spectrosc. Relat. Phenom. **18**, 1 (1980).
[15] E. F. Aziz, J. Gråsjö, J. Forsberg, E. Andersson, J. Söderström, L. Duda, W. Zhang, J. Yang, S. Eisebitt, C. Bergström, et al., J. Phys. Chem. A **111**, 9662 (2007).
[16] J. Vinson, J. J. Kas, F. D. Vila, J. J. Rehr, and E. L. Shirley, Phys. Rev. B **85**, 045101 (2012).
[17] J. Vinson and J. J. Rehr, Phys. Rev. B **86**, 195135 (2012).
[18] K. C. Prince, M. Vondráček, J. Karvonen, M. Coreno, R. Camilloni, L. Avaldi, and M. de Simone, J. Electron Spectrosc. Relat. Phenom. **101-103**, 141 (1999).
[19] P. Giannozzi, S. Baroni, N. Bonini, M. Calandra, R. Car, C. Cavazzoni, D. Ceresoli, G. L. Chiarotti, M. Cococcioni, I. Dabo, et al., J. Phys.: Condens. Matter **21**, 395502 (2009).
[20] E. L. Shirley, Phys. Rev. B **54**, 16464 (1996).
[21] D. Prendergast and S. G. Louie, Phys. Rev. B **80**, 235126 (2009).
[22] S. Tinte and E. L. Shirley, J. Phys.: Condens. Matter **20**, 365221 (2008).
[23] P. Giannozzi, S. de Gironcoli, P. Pavone, and S. Baroni, Phys. Rev. B **43**, 7231 (1991).
[24] G. Onida, L. Reining, and A. Rubio, Rev. Mod. Phys. **74**, 601 (2002).
[25] F. Bruneval, N. Vast, and L. Reining, Phys. Rev. B **74**, 045102 (2006).
[26] X. Gonze, B. Amadon, P.-M. Anglade, J.-M. Beuken, F. Bottin, P. Boulanger, F. Bruneval, D. Caliste, R. Caracas, M. Cote, et al., Computer Phys. Commun. **180**, 2582 (2009).
[27] H. A. Levy and S. W. Peterson, Phys. Rev. **86**, 766 (1952).
[28] E. L. Wagner and D. F. Hornig, J Chem.l Phys. **18**, 296 (1950).
[29] T. Pylkkänen, V. M. Giordano, J.-C. Chervin, A. Sakko, M. Hakala, J. A. Soininen, K. Hämäläinen, G. Monaco, and S. Huotari, J. Phys. Chem. B **114**, 3804 (2010).
[30] K. Kurki-Suonio, M. Merisalo, A. Vahvaselkä, and F. K. Larsen, Acta Cryst. A **32**, 110 (1976).
[31] H. Yamashita, J. Phys. Soc. Japan **29**, 1391 (1970).
[32] B. Brena, D. Nordlund, M. Odelius, H. Ogasawara, A. Nilsson, and L. G. M. Pettersson, Phys. Rev. Lett. **93**, 148302 (2004).
[33] H. E. Swanson, N. T. Gilfrich, and M. I. Cook, Natl. Bur. Std. Circular 539 **7**, 4 (1957).
[34] Yu. N. Zhuravlev, N. G. Kravchenko, A. S. Poplavnoĭ, and F. A. Dzyubenko, Optics and Spectroscopy **92**, 185 (2002).
[35] E. M. Witko, W. D. Buchanan, and T. M. Korter, J. Phys. Chem. A **115**, 12410 (2011).
[36] C. S. Choi, J. E. Mapes, and E. Prince, Acta Cryst. B **28**, 1357 (1972).
[37] K. Gilmore and E. L. Shirley, J. Phys.: Condens. Matter **22**, 315901 (2010).
[38] S. Ismail-Beigi and S. G. Louie, Phys. Rev. Lett. **90**, 076401 (2003).
[39] K. A. Mäder and S. Baroni, Phys. Rev. B **55**, 9649 (1997).
[40] F. Gel'mukhanov and H. Ågren, Physics Reports **312**, 87 (1999).
[41] M. Fuchs and M. Scheffler, Comput. Phys. Commun. **119**, 67 (1999).
[42] N. Troullier and J. L. Martins, Phys. Rev. B **43**, 1993 (1991).
[43] J. P. Perdew and Y. Wang, Phys. Rev. B **45**, 13244 (1992).